Structural and biophysical investigation of the interaction of a mutant Grb2 SH2 domain (W121G) with its cognate phosphopeptide

SCHOLARONE™
Manuscripts

Structural and biophysical investigation of the interaction of a mutant Grb2 SH2 domain (W121G) with its cognate phosphopeptide

Danai Papaioannou[1], Sebastian Geibel[1,2], Micha B. A. Kunze[1,#],

Christopher W. M. Kay[1,3], and Gabriel Waksman[1,*]

1 Institute of Structural and Molecular Biology, UCL and Birkbeck, Malet Street, WC1E 7HX London, UK

2 Institute for Molecular Infection Biology, University of Würzburg, Josef-Schneider-Strasse 2, Haus D15, 97080 Würzburg, Germany

3 London Centre for Nanotechnology, 17-19 Gordon Street, London WC1H 0AH, UK

* to whom correspondence should be addressed

Present address: Structural Biology and NMR Laboratory, Department of Biology, University of Copenhagen, Ole Maaløes Vej 5, DK-2200 Copenhagen N, Denmark

Abstract

The adaptor protein Grb2 is a key element of mitogenetically important signaling pathways. With its SH2 domain it binds to upstream targets while its SH3 domains bind to downstream proteins thereby relaying signals from the cell membranes to the nucleus. The Grb2 SH2 domain binds to its targets by recognizing a phosphotyrosine (pY) in a pYxNx peptide motif, requiring an Asn at the +2 position C-terminal to the pY with the residue either side of this Asn being hydrophobic. Structural analysis of the Grb2 SH2 domain in complex with its cognate peptide has shown that the peptide adopts a unique β-turn conformation, unlike the extended conformation that phosphopeptides adopt when bound to other SH2 domains. TrpEF1 (W121) is believed to force the peptide into this unusual conformation conferring this unique specificity to the Grb2 SH2 domain. Using X-ray crystallography, electron paramagnetic resonance (EPR) spectroscopy, and isothermal titration calorimetry (ITC), we describe here a series of experiments that explore the role of TrpEF1 in determining the specificity of the Grb2 SH2 domain. Our results demonstrate that the ligand does not adopt a pre-organized structure before binding to the SH2 domain, rather it is the interaction between the two that imposes the hairpin loop to the peptide. Furthermore, we find that the peptide adopts a similar structure when bound to both the wild-type Grb2 SH2 domain and a TrpEF1Gly mutant. This suggests that TrpEF1 is not the determining factor for the conformation of the phosphopeptide.

Introduction

Src Homology 2 (SH2) domains are protein modules found in many signal transduction proteins. They mediate protein-protein interactions during signaling by specifically recognizing and binding to tyrosine-phosphorylated sites[1]. Although there have been extensive investigations aiming to understand how SH2 domains specifically recognize tyrosine-phosphorylated peptides (reviewed in Liu et al., 2012[2]), some aspects of the mechanism that controls the interactions of SH2 domains with their targets still remain to be explored. One case in point is the SH2 domain of the adaptor protein Grb2.

The Grb2 SH2 domain belongs to a small group of 18 SH2 domains that show a strong binding proclivity for an Asn residue at the +2 position C-terminal of the phosphotyrosine (pY), with the general binding motif being pYxNx, where x can be any hydrophobic residue[3]. The SH2 domains of the Grb2/Grap/Gads family and Grb7 have been identified to recognize the pYxNx motif *in vivo*[4,5,6,7]. In the conventional SH2 domain binding mode (exemplified by the SH2 domain of the Src kinase[8,9]), the phosphorylated peptide usually binds to the SH2 domain in an extended, linear, conformation; the phosphotyrosine (pY) binds to a distinct pocket termed the "pY-binding" pocket of the domain while the sequence of the residues adjacent to the pY mediates binding specificity. In the case of the archetypal SH2 domain of the Src kinase (Src SH2 domain), binding specificity is primarily mediated by the interactions between another distinct pocket in the SH2 domain termed the "+3 specificity determining region/pocket" and the ligand's third (+3) residue C-terminal to the pY. However, in the case of the Grb2 SH2 domain, structural analysis of the domain bound to its cognate peptide has disclosed a unique peptide conformation[10,11,12]. When bound to the Grb2 SH2 domain the peptide adopts a type I β-turn conformation, with the +2 Asn forming a network of hydrogen bonds with residues of the domain. The different binding mechanism of the Grb2 SH2 domain was attributed to the composition and structure of its EF loop (the naming of the secondary structures follows the nomenclature introduced by Eck et al, 1994[13]). For the Grb2 SH2 domain, a Trp at the EF1 position of the loop (W121 or TrpEF1) is considered to be the key residue for its specificity[10-12,14]. With its bulky sidechain, TrpEF1 appears to force

the peptide into the hairpin conformation exposing the +2 Asn prominently for binding[10,11,12].

The importance of TrpEF1 for the molecular recognition mechanism of the Grb2 SH2 domain has been demonstrated in several studies, the most detailed of which established that a mutation to Trp at the EF1 position of the Src SH2 domain resulted in the switch of its specificity to that of Grb2[14]. The Src SH2 domain binds preferentially to phosphopeptides with two Glu residues at the +1 and +2 positions and an Ile at the +3 position C-terminal to the pY (motif pYEEI)[3,15]. However, the introduction of a Trp at the EF1 position of the Src SH2 domain (ThrEF1Trp mutant) led to a 20-fold decrease in affinity for its pYEEI cognate peptide and to a 60-fold increase for a peptide containing the Grb2-specific pYVNV motif[14]. Moreover, the Src SH2 ThrEF1Trp domain mutant behaves biologically like a Grb2 SH2 domain would, restoring vulva induction in *C.elegans* with a vulvaless phenotype[14]. Co-crystallization of the ThrEF1Trp mutant Src SH2 domain with a pYVNV motif-containing phosphopeptide revealed a mode of binding similar to that of the wild-type Grb2 SH2 domain/pYVNV peptide interaction[16]. Superimposition of the wild-type Grb2 SH2 domain/pYVNV peptide complex with the ThrEF1Trp mutant Src SH2 domain/pYVNV complex showed that the TrpEF1 in both structures is capable of forming stabilizing interactions with the ligands, and as a result, the peptides in the two structures make identical interactions and form a similar β turn[16]. This was a groundbreaking finding in the study of the selectivity of SH2 domains suggesting that mutating a single residue is enough to switch the specificity of an SH2 domain.

In the study presented here, a mutant Grb2 SH2 domain, in which a far less bulky Gly replaced TrpEF1 (TrpEF1Gly), was constructed in order to further investigate the importance of the EF1 position for the specificity of the Grb2 SH2 domain. We hypothesized that the substitution of TrpEF1 by Gly would relieve the constraints that appear to impose a β-turn conformation on the phosphopeptide ligand, resulting in the peptide binding in an extended, linear, conformation as observed for most SH2 domain ligands. We co-crystallized the mutant Grb2 SH2 domain with the SpYVNVQ peptide, which represents the Grb2 binding site at Tyr-317 of the human Shc protein, a native target of the Grb2 SH2

domain. The structure revealed a domain-swapped dimer where, surprisingly, the peptide binds in a similar mode as in the wild-type Grb2 SH2 domain, indicating that a Trp at position EF1 is not required to force a turn conformation on the peptide. This surprising result was confirmed by investigating the interaction of the peptide with wild-type and mutant Grb2 SH2 domains in solution using Electron Paramagnetic Resonance (EPR) spectroscopy in conjunction with nitroxide spin-labeling[17,18]. The structure of the pYVNV motif-containing peptide alone was also investigated and found to be flexible suggesting that the bound turn conformation is indeed imposed by binding. Finally, in order to investigate the possibility that the TrpEF1Gly mutation of the Grb2 SH2 domain might have switched the binding specificity to that of Src, ITC experiments were performed on both mutant and wild-type SH2 domains of both Src and Grb2, the results demonstrating that i- a TrpEF1Gly mutation in the Grb2 SH2 domain reduces binding of its cognate peptide by only 10-fold and increases binding of the Src-specific pYEEI peptide by only 6-fold, ii- conversely, a ThrEF1Trp mutation in the Src SH2 domain results in only a modest affinity gain of about 7-fold to the Grb2-specific pYVNV peptide while decreasing affinity to its cognate pYEEI peptide by 6-fold. We thus conclude that the position EF1 in both Grb2 and Src SH2 domains only plays a minor role in both peptide conformation and binding specificity.

Results and Discussion

Crystal structure of the Grb2 SH2 TrpEF1Gly domain in a complex with a pYxNx motif-containing peptide

During the purification, both wild-type Grb2 SH2 domain and the TrpEF1Gly mutant eluted in a dimeric and monomeric state. The concentration of the two states was equal for the wild-type domain while the proportion of monomers was higher (80%) for the mutant (results not shown). In all the experiments described below, only the monomeric fraction was used. However, the crystal structure revealed a domain-swapped dimer, which agrees with previous findings that the domain-swapped dimer is metastable[19].

The complex of the Grb2 SH2 domain bound to the SpYVNVQ peptide crystallized with 32 molecules in the asymmetric unit; 16 SH2 domains forming 8 domain-swapped dimers with all binding sites being occupied by a phosphopeptide. The crystal structure contains the SH2 domain residues from Glu 54 to Gln 153 and the -1 Ser, pY, +1 Val, +2 Asn, +3 Val, +4 Gln residues of the peptide ligand. The domain-swapped area of each domain includes residues 122-153. Each swapped Grb2 SH2 domain has an environment essentially identical to the monomeric SH2 domain, consisting of two α-helices and 5 β-strands, ordered αββββα, forming a central anti-parallel β-sheet sandwiched between the α-helices (Figure 1A).

All 8 dimers have similar structures with root-mean square deviation (RMSD) on C^α positions upon superposition ranging between 0.5 and 1.5 Å. The two molecules of the dimers differ to a limited degree from each other with RMSD on C^α positions upon superposition of the two monomers ranging between 1.1 and 2.5 Å with the main differences being in the loop regions. The temperature factors of the residues that interact with the peptide in each monomer are similar. Here, we will describe only one dimer of the asymmetric unit corresponding to chains Y and Z in the PDB file.

The wild-type Grb2 SH2 domain has been crystalized in a domain-swapped mode previously[12,19,20,21]. The structure of the Grb2 SH2 TrpEF1Gly domain is comparable to the previously described structures with the main

Papaioannou et al. (2015)

variability found at the domain-swapped C-terminal part (alignment with 1FYR dimer[19], RMSD 2.8 Å).

The peptide recognition sites are formed by both molecules of the domain-swapped dimer and are accessible on opposite sides of the dimer (Figure 1A). The binding of the SpYVNVQ peptides to the domain-swapped mutant Grb2 SH2 domains follows the same principles as with the wild-type monomeric Grb2 SH2 domain. -1 Ser of the peptide forms hydrogen bonds with the positively charged guanidinium group of ArgαA2 (R67). The pY is inserted in the pY-binding pocket where it forms multiple stabilizing interactions with residues ArgαA2 (R67), ArgβB5 (R86), SerβB7 (S88), SerBC2 (S90) and SerβC3 (S96), which is in perfect agreement with what has been previously described in the literature[10,12] (Figure 1B). +1 Val displays Van der Waals interactions with PheβD5 (F108) and GlnβD3 (Q106) of the SH2 domain while its main chain amide group interacts with the carbonyl group of HisβD4 (H107) of the domain, as previously stated. +2 Asn interacts via two hydrogen bonds with the main chain carbonyl oxygen and amide proton of LysβD6 (K109) (Figure 1C) and forms a third hydrogen bond with the main chain carbonyl oxygen of Gly EF1 (G121). In the wild-type domain-swapped Grb2 SH2 domains that have been crystallized previously, TrpEF1 (W121) was engaged in no interactions with the peptide unlike in the Grb2 SH2 monomeric domain structure where it forms close contacts with +2 Asn of the ligand in all reported structures[12,19,20]. +3 Val does not interact with the SH2 domain and points to the solvent while the side chain carboxyl of +4 Gln interacts with the main chain amide proton of LysβF1 (K124) via a hydrogen bond.

The structure of a monomeric Grb2 SH2 domain with a peptide with the sequence PSpYVNVQN has been previously described (PDB entry code: 1JYR)[12]. This peptide and the peptide in the structure presented here (chain J) align well with an RMSD of 0.4Å (Figure 1, D and E) and adopt a similar conformation. A common characteristic of the phosphopeptides when in complex with the Grb2 SH2 domain is an intra-molecular hydrogen bond between the pY and the +3 residue. In the mutant Grb2 SH2 domain/SpYVNVQ complex, the formation of a similar hydrogen bond is likely since the distance between the main-chain oxygen of pY and the main-chain nitrogen of the +3 Val is 3.17Å. However, the

torsion angles φ and ψ of the +2 Asn (-98.07 and 30.84) differ from the typical I β-turn torsion angles (-90 and 0) forcing the peptide to adopt a more twisted conformation. A similar peptidic conformation has been previously observed in the binding of a CD28-derived peptide, with the pYMNM sequence, to the wild-type Grb2 SH2 domain[22].

EPR spectroscopy of the interaction of the Grb2 SH2 domain with its cognate binding motif

We used EPR spectroscopy in order to obtain structural information for the interaction of the wild-type Grb2 SH2 and the TrpEF1Gly Grb2 SH2 domains with the pYVNV peptide in solution. For the experiments, a peptide with two cysteine residues at the N- and C-terminus, respectively, was used (sequence CSpYVNVQC). The covalent modification of this peptide with two nitroxide spin labels using a monobromo-maleimide spin label is described in the Materials and Methods section. Line broadening in continuous-wave (cw)-EPR spectroscopy experiments at ambient temperature confirmed the interaction of the labeled peptide with both the wild-type and the mutant Grb2 SH2 domains (Figure 2A). Binding of the peptide was observed via line broadening and a reduced high-field peak intensity of the bound form(s) when compared to the apo form (Figure 2A). EPR distance measurements using the 4-pulse DEER sequence[23] of both the Grb2 SH2 domain wild type and the Grb2 SH2 domain TrpEF1Gly mutant in a complex with the CSpYVNVQC peptide showed that the distance of the two spins for the major population of the peptide was between 1 and 3 nm (Figure 2, C and D). Modeling of the labels to the CSpYVNVQC peptide (PDB code: 1JYR[12]) using the Maestro program (Schrödinger, LLC, New York, NY) predicted a distance of 1.86 nm (18.6 Å) between the two labels (Figure 2B), which is consistent with the distances obtained from the DEER experiments.

These data indicate that the peptide behaves in a comparable way when bound to both the wild-type and the Grb2 SH2 domain mutant confirming the crystallography data that a Trp residue at position EF1 is not the determining factor for the conformation of the phosphopeptide, as has been previously suggested[10,12].

An EPR distance measurement was also recorded for the free peptide in solution (Figure 2, C and D). According to our data, when free in solution, the CSpYVNVQC peptide presents high mobility and adopts a wide range of conformations leading to a far broader distance distribution than for the bound-peptides. Note that spin-spin distances smaller than 1.5 nm are also likely to be present, but can not be directly observed by DEER as indicated by the dotted lines in Figure 2D. This result demonstrates that the ligand does not adopt a pre-organized structure before binding to the SH2 domain and it is the interaction between the two that imposes the hairpin loop to the peptide.

ITC analysis of Src and Grb2 wild-type and mutant SH2 domains with their cognate peptides

ITC experiments were employed to probe the binding properties of both the wild-type and the Grb2 SH2 TrpEF1Gly domains to the Grb2-specific SpYVNVQ ligand and the PQpYEEIPI (Src-specific) ligand (Table 1). The substitution of the TrpEF1 by a Gly led to a ~10-fold loss in the binding affinity to the SpYVNVQ peptide mainly attributed to a lower binding enthalpy (~30% less). The wild-type Grb2 SH2 domain bound with a low affinity to the PQpYEEIPI peptide ($Kd=167\mu M$), indicating that this is not a specific interaction. The removal of the bulky side chain of the TrpEF1 increased the affinity of the Grb2 SH2 domain for the PQpYEEIPI peptide by only ~6-fold, suggesting that the removal of the aromatic TrpEF1 is not sufficient for the Grb2 SH2 domain to switch specificity to the PQpYEEIPI peptide.

The wild-type Src SH2 domain was shown to bind to the PQpYEEIPI peptide with a dissociation constant (*Kd*) of 0.22 μM. The measured affinity agrees with published data (*Kd*= 0.18 μM[24]). Moreover, the Src SH2 domain bound to the SpYVNVQ peptide with a *Kd* of 8 μM; ~40-fold lower than the affinity for the PQpYEEIPI peptide. Inserting a Trp at the corresponding EF1 position of Src SH2 domain (Src SH2 ThrEF1Trp mutant) resulted in a similar binding affinity for both the PQpYEEIPI and SpYVNVQ peptides (*Kd*= 1.3 and 1.1 µM, respectively). The affinity of the Src SH2 domain ThrEF1Trp was decreased by ~6-fold for the PQpYEEIPI peptide but increased by ~7-fold for the SpYVNVQ peptide when compared to the wild-type. The interaction with both peptides was

entropically driven. The decrease in affinity for the PQpYEEIPI peptide is readily explicable from the structure, as the indole ring of the Trp residue sterically prevents the interaction of the peptide's +3 residue with the specificity-binding pocket[16]. Moreover, the increase in the binding affinity of the Src SH2 ThrEF1Trp domain for the SpYVNVQ peptide could be partially explained from the Van der Waals bonds that TrpEF1 forms with the +2 Asn of the peptide[16]. These results differ from previously published data where, in SPR experiments, the specific point mutation of the Src SH2 domain led to a 20-fold decrease in affinity for a pYEEI-containing motif peptide (sequence EPQpYEEIPIYLK) and to a 60-fold increase for a pYVNV-containing peptide (sequence DPSpYVNVQNLDK)[14].

Conclusion

The Grb2 SH2 domain has previously been shown to bind specifically to tyrosine-phosphorylated peptides with the pYxNx motif. Such peptides adopt a characteristic type I β-turn upon binding. This unique peptide conformation has been attributed to a Trp at the EF1 position of the SH2 domain, which is only found in the Grb2 SH2 domain and the closely related Grap and Gads SH2 domains. In our study, a Grb2 SH2 domain mutant where TrpEF1 is substituted to Gly binds to the pYVNV motif-containing ligand by forming a similar network of interactions as has been described for the wild-type Grb2 SH2 domain, suggesting that a Trp at this position does not impose constraints on the conformation of the peptide ligand. EPR analysis confirms that, in the bound state, the conformation of the peptide is the same whether bound to the wild-type and mutant SH2 domains, a conclusion reinforced by ITC results. These also indicate that Trp at position EF1 plays a much less important role than previously suggested as the reduction in affinity is only 10-fold compared to wild-type.

The pYVNV motif-containing peptide forms most of its interactions with the main chain atoms of the Grb2 SH2 domain, suggesting that any SH2 domain using its backbone hydrogen bonding capabilities could bind to some extent to a peptide with the pYxNx motif. This explains why the Src SH2 ThrEF1Trp domain binds with relatively high affinity to the SpYVNVQ peptide (this study and [14,16]). However, the increased affinity of the Src SH2 ThrEF1Trp domain for the

SpYNVNQ peptide is, in our hands, much less pronounced than previously reported: a 7-fold increase compared to a 60-fold increase by Marengere et al. (1994)[14]. There is no structural evidence of the binding of the wild-type Src SH2 domain to a peptide bearing the pYxNx motif, but molecular dynamics simulations have suggested that a pYxNx motif-containing peptide would also adopt a β-turn conformation when bound to the Src SH2 domain[25]. In the same study the free energy of binding of the Src SH2 domain to a pYVNV motif-containing peptide was estimated using fluorescent polarization binding assays to be -29.1 kJ/mol, which is in excellent agreement with the free energy measured in the ITC experiments reported here (ΔG = -29.08 kJ/mol). Consistent with these data, *in vivo* targets of Grb2 and Src SH2 domains have been identified where both domains recognize the same sequence[26,27].

Key to SH2 domain binding thermodynamics is the conformation of the peptide ligand in its unbound state[28,29]. It has been suggested that decreasing conformational sampling might lower the entropic cost of binding. Studies have suggested that the SpYVNVQ peptide might be able to adopt a β-turn conformation in solution but the EPR data presented here suggest it does not and is instead conformationally flexible, implying a entropic cost component to its binding thermodynamics.

Detailed studies of Src SH2 domain binding thermodynamics have all pointed to the fact that the range of affinities within which SH2 domains appear to operate is relatively narrow. Until now, the Grb2 SH2 domain appeared to be an exception. However, our study demonstrates that this is not the case. Instead, our data confirm that the binding specificity of SH2 domains, even that of Grb2, results from multiple factors and does not depend merely on the nature of one particular residue.

Materials and Methods

DNA constructs.

The Grb2 SH2 domain in the pQE-60 vector was provided from Dr Stephen F. Martin (University of Texas at Austin, TX, USA). The Src SH2 domain, in the pET-3a plasmid, was as described in Waksman et al., 1992[8].

Peptides

The peptides used in this study were synthesized by Biosynthesis Inc (Lewisville, TX). The sequences of the peptides that are described in this study are the following; SpYVNVQ: Ac-S(pY)VNVQ-CONH2, CSpYVNVQC: Ac-CS(pY)VNVQC-CONH2, PQpYEEIPI: Ac-PQ(pY)EEIPI-CONH2. The purity of the peptides was assessed by HPLC and ESI-MS. The extinction coefficient used was determined as described by Bradshaw et al., 1998[30].

Site-directed mutagenesis

All mutagenesis was carried out using the QuikChange protocol (Stratagene, 2004), a PCR-based technique for site- directed mutagenesis. Forward and reverse mutagenic oligonucleotide primers were designed in accordance with the QuikChange protocol (Table 2). The KOD Hot Start DNA Polymerase (Novagen) was used in all the mutagenesis experiments.

Protein Purification

Ni-NTA chromatography was used for the purification of the Grb2 SH2 domain constructs. The cells expressing the 6His-tagged proteins were lysed in 0.1 M Sodium Phosphate pH 7.2, 300 mM NaCl, 50 mM Imidazole. After clarification the lysate was passed through a 5 ml Ni-NTA Superflow column (Qiagen), connected to an AKTA Prime (GE Healthcare), at a flow rate of 1.5 ml/min. The column was washed using 10 column volumes of the binding buffer and the Grb2 SH2 domain constructs were eluted using 300 mM Imidazole, 0.1M Sodium Phosphate pH 7.2, 300 mM NaCl. Fractions containing the 6His-tagged SH2 domains were identified using SDS-PAGE gels, pooled and concentrated.

For the Src SH2 domain constructs, the cells were lysed in 0.1 M Sodium Phosphate pH 7.0, 1 mM EDTA, 5 mM DTT and after clarification the lysate was applied to an SP- sepharose column (GE Healthcare) connected to an AKTA Prime. Bound proteins were eluted using a 0-1M NaCl gradient. Fractions containing the SH2 domain constructs were identified using SDS-PAGE gels, pooled and concentrated.

After the first purification step the eluent was concentrated to 2-3 mls using Amicon centrifuge devices with a 3 kDa cut-off and then loaded to a prepacked Sephacryl S-100 column (GE Healthcare) using an AKTA Prime system. The column was pre-equilibrated in a gel filtration buffer, the composition of which was dependent on the type of experiments the samples were subsequently subjected to, and run at 0.8 ml/min. Fractions containing the appropriate peaks, as assessed by SDS-PAGE, were pooled and concentrated.

Crystallization experiments

Grb2 SH2 TrpEF1Gly domain with a C-terminal 6His-tag was purified by affinity and size exclusion chromatography and its purity was assessed by SDS-PAGE. Before setting up crystal trials the buffer of the protein was exchanged to 50 mM Sodium Cacodylate pH 6.5 by ultrafiltration using Amicon centrifugation devices with 3 kDa cut-off. The protein was then concentrated to ~20-40 mg/ml. The SpYVNVQ peptide was dissolved in the same buffer and added to the protein at a 1:1.5 molar ratio.   Crystallization experiments were performed by vapour diffusion using the hanging drop method with reservoirs containing 0.2 M Sodium Thiocyanate, Potassium Thiocyanate between 0.31 M to 0.3975 M, and the PEG-8000 between 28% to 33% (w/v)). The optimal crystals were grown at 0.335 M Potassium thiocyanate, 31% (w/v) PEG 8000. Crystals and cryoprotectants were tested with the in house Rigaku RA-Micro7 HFM tabletop rotating anode X-ray generator. Datasets were collected at the beamline ID29 at the ESRF synchrotron radiation facility in France and at the Proxima1 microfocus beamline with an ADSC Quantum 315r CCD detector at the SOLEIL synchrotron radiation facility in France.

Images were processed using the XDS software package[31]. BALBES[32] was used for molecular replacement and ligand building and structure manipulation

was achieved using Coot[33] and PHENIX[34] (see Table 3 for data collection and final refinement statistics).

EPR Spectroscopy

Spin-Labeling.

Labeling of the CSpYVNVQC peptide was attempted with MTSSL (Sigma-Aldrich) according to standard protocols. However, labeling resulted in greatly reduced solubility and thus a monobromo-maleimide (3-bromo-2,5-dioxo-2,5-dihydro-pyrrole-1-carboxylic acid methyl ester) spin label was synthesized in analogy to the dibromo-maleimide (3,5-dibromo-2,5-dioxo-2,5-dihydro-pyrrole-1-carboxylic acid methyl ester) described in Schumacher et al. 2013[35].

The label was dissolved in 100% DMF at a concentration of 10 mM and was added in 0.2 mM of peptide (20 mM Hepes pH 7.5, 150 mM NaCl, 5 mM EDTA) to reach a 1:2 peptide/label molar ratio. The reaction was incubated at room temperature for 2 hours in the dark. The labeling was assessed using ESI-MS and the yield calculated to be 97%.

Cw-EPR.

The protein (200 μM) was mixed with the peptide (1:0.5 ratio of protein: peptide, to ensure that all the peptide molecules are in a bound state) in 20 mM Hepes pH 7.5, 150 mM NaCl. Cw-EPR experiments at ambient temperature were performed on a EMXPlus EPR spectrometer (Bruker Biospin) operating at X-Band (9.7 GHz, 0.3 T) equipped with a 4122SHC resonator. All measurements were carried out with 2 mW microwave power, 100 kHz modulation frequency, 0.1 mT modulation amplitude and 20 ms conversion time and time constant.

EPR distance measurements.

The protein (50 μM) was mixed with the peptide (1:0.5 ratio of protein) in 20 mM Hepes at pH 7.5, 150 mM NaCl. 5% glycerol was added and the samples were frozen in liquid N_2. Experiments were performed at 50 K on an ELEXSYS E580 EPR spectrometer (Bruker Biospin) operating at X-Band (9.2 GHz, 0.3 T) equipped with an ER-4118-X-MS-3W resonator. The four-pulse DEER sequence[21] was chosen with $\pi/2_{obs} - \tau 1 - \pi_{obs} - (\tau 1 + t) - \pi_{pump} - (\tau 2 - t) - \pi_{obs} - \tau 2 - echo$, where the observer pulse length was 16 ns for $\pi/2$ and 32 ns for π pulses. The pump pulse length was 12 ns, the long interpulse delay was t = 2 μs. All other

parameters were used according to Pannier et al., 2000[23]. The DEER spectra were analyzed using the program DeerAnalysis2014[36]. The dipolar evolution was background-corrected by assuming a homogeneous three-dimensional distribution. The distance distributions obtained were checked for stability according to the DeerAnalysis2010 manual.

ITC

The ITC experiments described in this study were performed on a VP-ITC Microcalorimeter (Malvern Instruments, Malvern, UK). The protein samples were concentrated to 50-100 μM and dialyzed extensively against 20 mM Hepes pH 7.5, 100 mM NaCl. The peptides were dissolved to a concentration of ~0.5-1.5 mM in the same buffer. In order to reduce errors arising from heats of dilution due to buffer differences between the samples in the syringe and the reaction vessel, the peptides were dialyzed against the same buffer used with the proteins. Both peptide and protein concentrations were determined using measured A280 values. The experimental concentration of the protein was taken as 98% of the calculated value (in accordance with manufacturers recommendations) to account for dilution from residual buffer in the cell. Samples of protein, peptide and dialysis buffer were degassed for 10 minutes at 25 °C prior to the experiment. The reference power was set to 10 μCal/sec and the cell contents were stirred continuously at 25°C and 310 rpm in order to ensure sufficient mixing while keeping baseline noise at a minimum. The injection sequence consisted of an initial 2μl injection to prevent artifacts arising from the filling of the syringe, followed by 35 x 8μl injections until final saturation was observed and the heat changes were monitored. A binding isotherm was generated by plotting the heat change of each injection against the molar ratio of the ligand to the protein. Using Origin (Malvern Instruments, Malvern, UK) a binding isotherm was fit by a single binding site model using a non-linear least squares method. During the fitting, all the parameters were allowed to float. In the experiments with low binding affinity, c<20, the curve fitting becomes over parameterized and, thus, the stoichiometry was set to 1 leaving only two variable parameters for fitting[37]. Data were corrected for heats of dilution before further analysis, by subtracting the basal heat that remained

following saturation. From the nonlinear least squares fit of the binding curve the stoichiometry n of the binding (ligand:protein), the equilibrium binding constant Ka and the change in enthalpy ΔH were defined. The change in free energy ΔG was calculated from Equation $\Delta G = \Delta H - T\,\Delta S$. Dissociation constant values (Kd) were calculated as the reciprocal of the observed binding constant (Kd = 1/ Ka).

Papaioannou et al. (2015)

Table 1. Thermodynamical analysis of the Grb2 and Src constructs interactions with the SpYVNVQ and PQpYEEIPI peptides.

Isothermal titration calorimetry data for the binding of the SpYVNVQ and PQpYEEIPI peptides to the wild-type Grb2 and Src SH2 domains as well as the Grb2 SH2 TrpEF1Gly and Src SH2 ThrEF1Trp domains. ITC experiments were conducted in duplicates at 25 °C with the same batch of ligand and in HEPES at pH 7.5. Uncertainties represent deviations from the average.

SH2 domain	Stoichiometry (n)	Kd (µM)	ΔG (kJ mol^{-1})	ΔH (kJ mol^{-1})	$-T\Delta S$ (kJ mol^{-1})
SpYVNVQ					
Grb2 SH2 wt	1.1±0.1	0.3±0.1	-37.3±0.1	-31.4±1.0	-5.9±1.1
Src SH2 wt	0.9±0.1	8.0±0.1	-29.1 ±0.1	-12.4±6.2	-16.7±6.2
Grb2 SH2 TrpEF1Gly	1.1±0.1	2.9±0.4	-31.6±0.3	-20.8±0.1	-10.9± 0.2
Src SH2 ThrEF1Trp	1.2±0.1	1.1±0.1	-34.0±0.2	-13.1±0.1	-20.9±0.1
PQpYEEIPI					
Grb2 SH2 wt	1.0±0.1	167.8±31.1	-21.6±0.5	-29.5±8.8	7.9±9.3
Src SH2 wt	1.1±0.2	0.2±0.1	-38.0±2.5	-24.1±1.9	-13.9±2.3
Grb2 SH2 TrpEF1Gly	0.9±0.1	27.8±1.0	-26.0±0.1	-18.5±2.8	-7.5±2.8
Src SH2 ThrEF1Trp	1.0±0.1	1.3±0.3	-33.5±0.6	-11.1±1.2	-22.4±1.8

Table 2: Oligonucleotide primer sequences used in this study

Mutation	Name of Primer	Sequence of primer
Grb2 SH2 TrpEF1Gly	W121Ggrb2-fw	5' GGG AAG TAC TTC CTC GGA GTG GTG AAG TTC AAT TC 3'
	W121Ggrb2-rv	5' GA ATT GAA CTT CAC CAC TCC GAG GAA GTA CTT CCC 3'
Src SH2 ThrEF1Trp	T225W-fw	5' GC GGC TTC TAC ATC TGG TCA CGC ACA CAG TTC 3'
	T225W-rv	5' GAA CTG TGT GCG TGA CCA GAT GTA GAA GCC GC 3'

Table 3. Statistics for data collection and structure refinement

	Grb2 SH2 domain (W121G) / pYVNV peptide complex
Data collection	
Space group	$P12_11$
Cell dimensions	
a, b, c (Å)	82.6, 72.1, 172.1
α, β, γ (°)	90.0, 93.3, 90.0
Resolution (Å)	41.3 – 2.6
R_{sym} (%) [a]	8.0 (61.4)
I/σI	12.0 (2.2)
Completeness (%)	98.9 (93.1)
Total reflections	230816
Unique reflections	62044
Multiplicity	3.7 (3.4)
Refinement	
Resolution (Å)	41.3 – 2.6
R_{work}/R_{free} [b, c]	23.6/29.4
No. atoms	13190
Ligand/ion	0
Water	99
B-factors ($Å^2$)	
Wilson B	51.5
Protein average	58.5
R.m.s deviations	
Bond lengths (Å)	0.002
Bond angles (°)	0.6
Ramachandran favored (%)	96.3
Ramachandran allowed (%)	3.6
Ramachandran outliers (%)	0
Molprobity[38]	
Clashscore (100th percentile)*	2.1
Overall score (100th percentile)*	1.2

[a] $R_{sym} = \Sigma|I - <I>|/\Sigma<I>$, where I is the observed and $<I>$ is the average intensity of the given reflection.

[b] $R_{work} = \Sigma_{hkl} ||F_{obs}| - |F_{calc}|| / \Sigma_{hkl} |F_{obs}|$.

[c] R_{free} is defined as above but calculated for 5% of reflections randomly excluded from the refinement.

Numbers in parentheses are for the highest resolution shell (2.6-2.7 Å).

* 100th percentile is the best among structures of comparable resolution; 0th percentile is the worst.

Papaioannou et al. (2015)

References

1. Moran MF, Koch CA, Anderson D, Ellis C, England L, Martin GS, Pawson T (1990) Src homology region 2 domains direct protein-protein interactions in signal transduction. Proc Natl Acad Sci U S A 87(21): 8622-8626.

2. Liu BA, Engelmann BW, Nash PD (2012) The language of SH2 domain interactions defines phosphotyrosine-mediated signal transduction. FEBS Lett 586(17): 2597-2605.

3. Huang H, Li L, Wu C, Schibli D, Colwill K, Ma S, Li C, Roy P, Ho K, Songyang Z, Pawson T, Gao Y, Li SS (2008) Defining the specificity space of the human SRC homology 2 domain. Mol Cell Proteomics 7(4): 768-784.

4. Rozakis-Adcock M, McGlade J, Mbamalu G, Pelicci G, Daly R, Li W, Batzer A, Thomas S, Brugge J, Pelicci PG, Schlessinger J, Pawson T (1992) Association of the Shc and Grb2/Sem5 SH2-containing proteins is implicated in activation of the Ras pathway by tyrosine kinases. Nature 360(6405): 689-692.

5. Yokote K, Margolis B, Heldin CH, Claesson-Welsh L (1996) Grb7 is a downstream signaling component of platelet-derived growth factor alpha- and beta-receptors. J Biol Chem 271(48): 30942-30949.

6. Liu SK, McGlade CJ (1998) Gads is a novel SH2 and SH3 domain-containing adaptor protein that binds to tyrosine-phosphorylated Shc. Oncogene 17(24): 3073-3082.

7. Feng GS, Ouyang YB, Hu DP, Shi ZQ, Gentz R, Ni J (1996) Grap is a novel SH3-SH2-SH3 adaptor protein that couples tyrosine kinases to the Ras pathway. J Biol Chem 271(21): 12129-12132.

8. Waksman G, Kominos D, Robertson SC, Pant N, Baltimore D, Birge RB, Cowburn D, Hanafusa H, Mayer BJ, Overduin M, Resh MD, Rios CB, Silverman L,

Kuriyan J (1992) Crystal structure of the phosphotyrosine recognition domain SH2 of v-src complexed with tyrosine-phosphorylated peptides. Nature 358(6388): 646-653.

9. Waksman G, Shoelson SE, Pant N, Cowburn D, Kuriyan J (1993) Binding of a high affinity phosphotyrosyl peptide to the Src SH2 domain: crystal structures of the complexed and peptide-free forms. Cell 72(5): 779-790.

10. Rahuel J, Gay B, Erdmann D, Strauss A, Garcia-Echeverría C, Furet P, Caravatti G, Fretz H, Schoepfer J, Grütter MG (1996) Structural basis for specificity of Grb2-SH2 revealed by a novel ligand binding mode. Nat Struct Biol 3(7): 586-589.

11. Ogura K, Tsuchiya S, Terasawa H, Yuzawa S, Hatanaka H, Mandiyan V, Schlessinger J, Inagaki F (1999) Solution structure of the SH2 domain of Grb2 complexed with the Shc-derived phosphotyrosine-containing peptide. J Mol Biol 289(3): 439-445.

12. Nioche P, Liu WQ, Broutin I, Charbonnier F, Latreille MT, Vidal M, Roques B, Garbay C, Ducruix A (2002) Crystal structures of the SH2 domain of Grb2: highlight on the binding of a new high-affinity inhibitor. J Mol Biol 315(5): 1167-1177.

13. Eck MJ, Shoelson SE, Harrison SC (1993) Recognition of a high-affinity phosphotyrosyl peptide by the Src homology-2 domain of p56lck. Nature 362(6415): 87-91.

14. Marengere LE, Songyang Z, Gish GD, Schaller MD, Parsons JT, Stern MJ, Cantley LC, Pawson T (1994) SH2 domain specificity and activity modified by a single residue. Nature 369(6480): 502-505.

15. Songyang Z, Shoelson SE, Chaudhuri M, Gish G, Pawson T, Haser WG, King F, Roberts T, Ratnofsky S, Lechleider RJ, Neel BG, Birge RB, Fajardo JE, Chou MM, Hanafusa H, Schaffhausen B, Cantley LC (1993) SH2 domains recognize specific

phosphopeptide sequences. Cell 72(5):767-778.

16. Kimber MS, Nachman J, Cunningham AM, Gish GD, Pawson T, Pai EF (2000) Structural basis for specificity switching of the Src SH2 domain. Mol Cell 5(6): 1043-1049.

17. Jeschke G (2012) DEER Distance Measurements on Proteins. Annu Rev of Phys Chem 63: 419-446.

18. Klare JP (2013) Site-directed spin labeling EPR spectroscopy in protein research. Biol Chem 394(10):1281-1300.

19. Schiering N, Casale E, Caccia P, Giordano P, Battistini C (2000) Dimer formation through domain swapping in the crystal structure of the Grb2-SH2-Ac-pYVNV complex. Biochemistry 39(44): 13376-13382.

20. Benfield AP, Whiddon BB, Clements JH, Martin SF (2007) Structural and energetic aspects of Grb2-SH2 domain-swapping. Arch Biochem Biophys 462(1): 47-53.

21. Phan J, Shi ZD, Burke TR Jr, Waugh DS (2005) Crystal structures of a high-affinity macrocyclic peptide mimetic in complex with the Grb2 SH2 domain. J Mol Biol 353(1): 104-115.

22. Higo K, Ikura T, Oda M, Morii H, Takahashi J, Abe R, Ito N (2013) High resolution crystal structure of the Grb2 SH2 domain with a phosphopeptide derived from CD28. PLoS One 8(9): e74482.

23. Pannier M, Veit S, Godt A, Jeschke G, Spiess HW (2000) Dead-time free measurement of dipole-dipole interactions between electron spins. J Magn Reson 142(2):331-340.

24. Bradshaw JM, Mitaxov V, Waksman G (1999) Investigation of

phosphotyrosine recognition by the SH2 domain of the Src kinase. J Mol Biol 293(4): 971-985.

25. Nachman J, Gish G, Virag C, Pawson T, Pomès R, Pai E (2010) Conformational determinants of phosphotyrosine peptides complexed with the Src SH2 domain. PLoS One 5(6): e11215.

26. Ponzetto C, Bardelli A, Zhen Z, Maina F, dalla Zonca P, Giordano S, Graziani A, Panayotou G, Comoglio PM (1994) A multifunctional docking site mediates signaling and transformation by the hepatocyte growth factor/scatter factor receptor family. Cell 77(2): 261-271.

27. Zheng XM, Resnick RJ, Shalloway D (2002) Mitotic activation of protein-tyrosine phosphatase alpha and regulation of its Src-mediated transforming activity by its sites of protein kinase C phosphorylation. J Biol Chem 277(24): 21922-21929.

28. Davidson JP, Lubman O, Rose T, Waksman G, Martin SF (2002) Calorimetric and structural studies of 1,2,3-trisubstituted cyclopropanes as conformationally constrained peptide inhibitors of Src SH2 domain binding. J Am Chem Soc 124(2): 205-215.

29. Delorbe JE, Clements JH, Whiddon BB, Martin SF (2010) Thermodynamic and Structural Effects of Macrocyclization as a Constraining Method in Protein-Ligand Interactions. ACS Med Chem Lett 1(8): 448-452.

30. Bradshaw JM, Waksman G (1998) Calorimetric investigation of proton linkage by monitoring both the enthalpy and association constant of binding: application to the interaction of the Src SH2 domain with a high-affinity tyrosyl phosphopeptide. Biochemistry 37(44): 15400-15407.

31. Kabsch W (2014) Processing of X-ray snapshots from crystals in random orientations. Acta Crystallogr D Biol Crystallogr 70(Pt 8): 2204-2216.

Papaioannou et al. (2015)

32. Long F, Vagin AA, Young P, Murshudov GN (2008) BALBES: a molecular-replacement pipeline. Acta Crystallogr D Biol Crystallogr 64(Pt 1):125-32

33. Emsley P, Cowtan K (2004) Coot: model-building tools for molecular graphics. Acta Crystallogr D Biol Crystallogr 60(Pt 12 Pt 1): 2126-2132.

34. Adams PD, Grosse-Kunstleve RW, Hung LW, Ioerger TR, McCoy AJ, Moriarty NW, Read RJ, Sacchettini JC, Sauter NK, Terwilliger TC. (2002) PHENIX: building new software for automated crystallographic structure determination. Acta Crystallogr D Biol Crystallogr 58: 1948-1954.

35. Schumacher FF, Sanchania VA, Tolner B, Wright ZVF, Ryan CP, Smith MEB, Ward JM, Caddick S, Kay CWM, Aeppli G, Chester KA & Baker JR (2013) Homogeneous antibody fragment conjugation by disulfide bridging introduces "spinostics." Scientific Reports 3:1525.

36. Jeschke G, Chechik V, Ionita P, Godt A, Zimmermann H, Banham J, Timmel CR, Hilger D, Jung H (2006) DeerAnalysis2006—a comprehensive software package for analyzing pulsed ELDOR data. Appl Magn Reson 30: 473-498.

37. Turnbull WB, Daranas AH (2003) On the value of c: can low affinity systems be studied by isothermal titration calorimetry? J Am Chem Soc 125(48): 14859-14866.

38. Chen VB, Arendall WB 3rd, Headd JJ, Keedy DA, Immormino RM, Kapral GJ, Murray LW, Richardson JS, Richardson DC (2010) MolProbity: all-atom structure validation for macromolecular crystallography. Acta Crystallogr. D Biol. Crystallogr 66 (Pt 1):12–21.

Figure legends

Figure 1. The structure of the Grb2 SH2 TrpEF1Gly dimer in complex with the SpYVNVQ peptide. (A) Structure of a domain-swapped dimer in complex with their phosphopeptide ligands. Each SH2 domain is in ribbon representation color-coded in cyan and magenta. Peptides are shown in sticks representation color-coded in yellow, red, orange and blue for carbon, oxygen, phosphorus and nitrogen atoms, respectively. The main secondary structures of the SH2 domain are labelled in black while the residues in the peptide are labelled in yellow. (B) The interactions between the phosphotyrosine (pY) and the SH2 domain. The main-chain trace of the SH2 domain is shown as cyan ribbon representation with the side-chains of some key residues shown in sticks representation. The phosphopeptide is shown in sticks representation. The dashed lines indicate hydrogen bonds. Color-coding of atoms and labelling of residues are as in A. (C) The interactions of the +2 Asn of the peptide and the SH2 domain. SH2 domain, peptide ligands, labelling and H-bonds are representated and indicated as in C. (D and E) Superposition of 2 peptides bound to Grb2 SH2. The SH2 domain is shown as grey ribbon, whereas the phosphopeptides are shown as sticks representation, color-coded red for the SpYVNVQ peptide ligand of the present work, and green for a pYVNV-containing motif peptide (sequence PSpYVNVQN) bound to the wild-type Grb2 SH2 domain determined by Nioche et al. 2002[12] (PDB entry code 1JYR). Orientation in D and E are similar to that in C and A, respectively.

Figure 2. EPR analysis of the binding of the wild-type and mutant Grb2 SH2 domains to the CSpYVNVQC peptide variant. (A) CW-EPR spectra of the peptide alone (blue; CSpYVNVQC), the Grb2 SH2 domain/CSpYVNVQC complex (red; Grb2 wt CSpYVNVQC) and the Grb2 SH2 TrpEF1Gly domain/CSpYVNVQC complex (amber; Grb2 TrpEF1Gly (W121G) CSpYVNVQC). The CW-spectra mainly provide information about the mobility of the spin labels and thus about the local environment of the labeled residues. In the spectra of the bound peptide, line broadening is observed in comparison with the apo peptide. This is evident in the decrease in relative intensity of the high-field peak. This effect

arises from the restriction of the peptide when bound to the Grb2 SH2 domains. (B) Stick representation of the modeled CSpYVNVQC peptide labeled with two bromo-maleimide nitroxide spin labels. The nitroxide spin labels were modeled using the Maestro program (Schrödinger). The red dots represent the static distance between the two NO moieties of the labels. (C) Dipolar evolution of the DEER measurements. Color code corresponds is the same as in (A). (D) Corresponding distance distributions of the dipolar evolution function of the three measurements shown in (C). The broader distance distribution of the apo peptide in comparison to the bound peptides is apparent. A dashed gray line signifies the modeled spin-spin distance of the labeled peptide when bound to Grb2 SH2.

Figure 3. ITC measurements of the Grb2 SH2 TrpEF1Gly domain binding to the SpYVNVNQ peptide (left) and the PQpYEEIPI peptide (right). Top panels show the raw data titration and lower panels show the data and best-fit curves obtained from data analysis using a single site model.

Figure 1   Papaioannou et al. (2015)
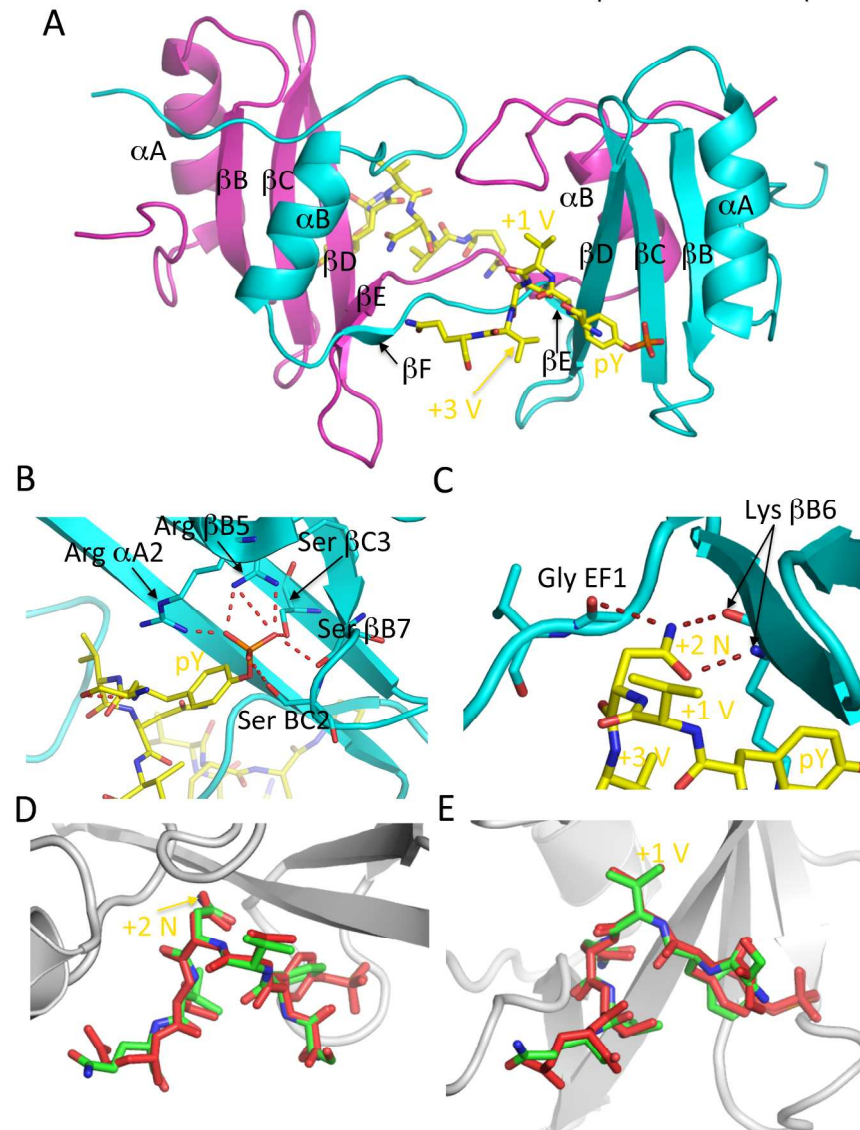
Figure 1
190x254mm (300 x 300 DPI)

Figure 2   Papaioannou et al. (2015)

Figure 2
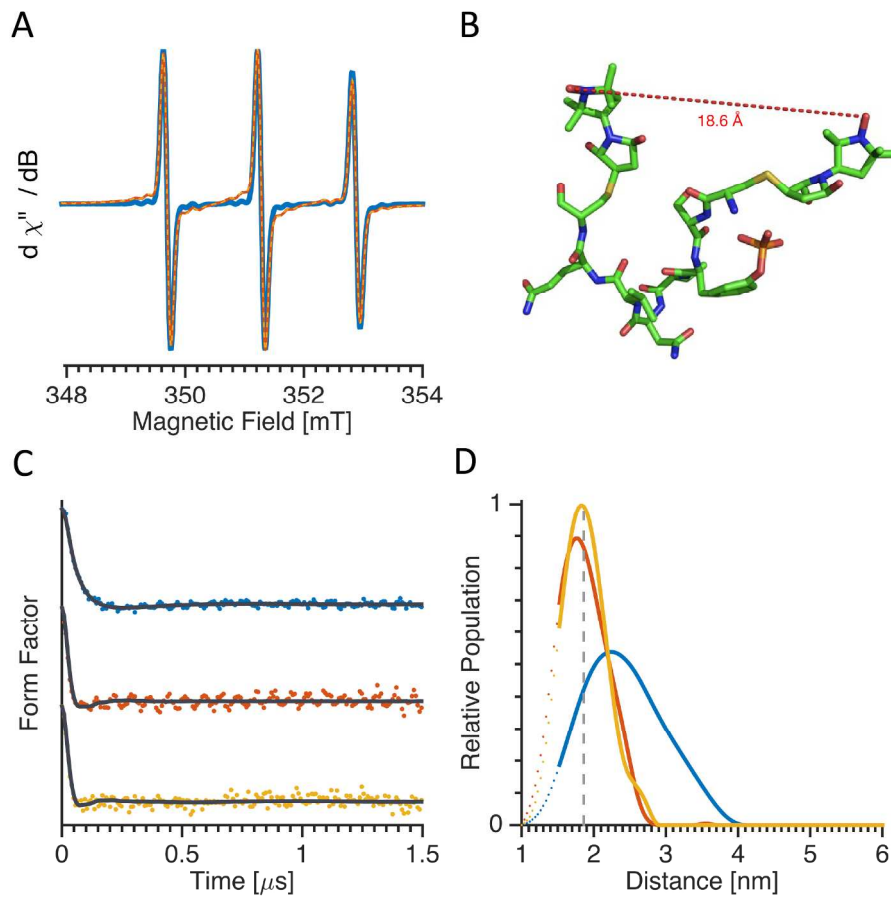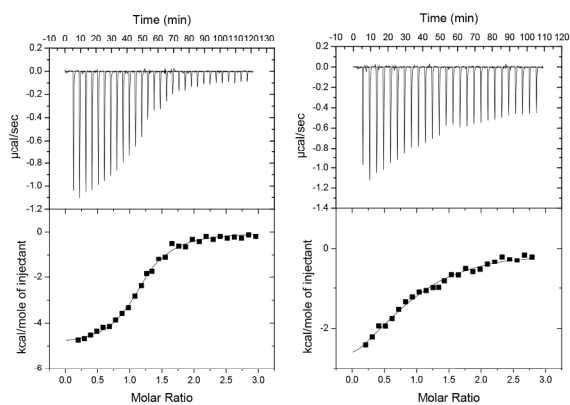190x254mm (300 x 300 DPI)

Figure 3   Papaioannou et al. (2015)

Figure 3
190x254mm (300 x 300 DPI)